Surfactant-Mediated Porous MOF-5 for High-Performance Triboelectric Nanogenerators

*Amaal Romih[1], Carmen Abuoudah[1], Andreas Schiffer[1,3], Vincent Chan[2,3], Lianxi Zheng[1,3]**

[1]Department of Mechanical and Nuclear Engineering, Khalifa University of Science and Technology, Abu Dhabi 127788, United Arab Emirates
[2]Department of Biomedical Engineering & Biotechnology, Khalifa University of Science and Technology, Abu Dhabi 127788, United Arab Emirates
[3]Research and Innovation Centre for Graphene and 2D Materials (RIC-2D), Khalifa University of Science and Technology, Abu Dhabi 127788, United Arab Emirates

**For correspondence: lianxi.zheng@ku.ac.ae*

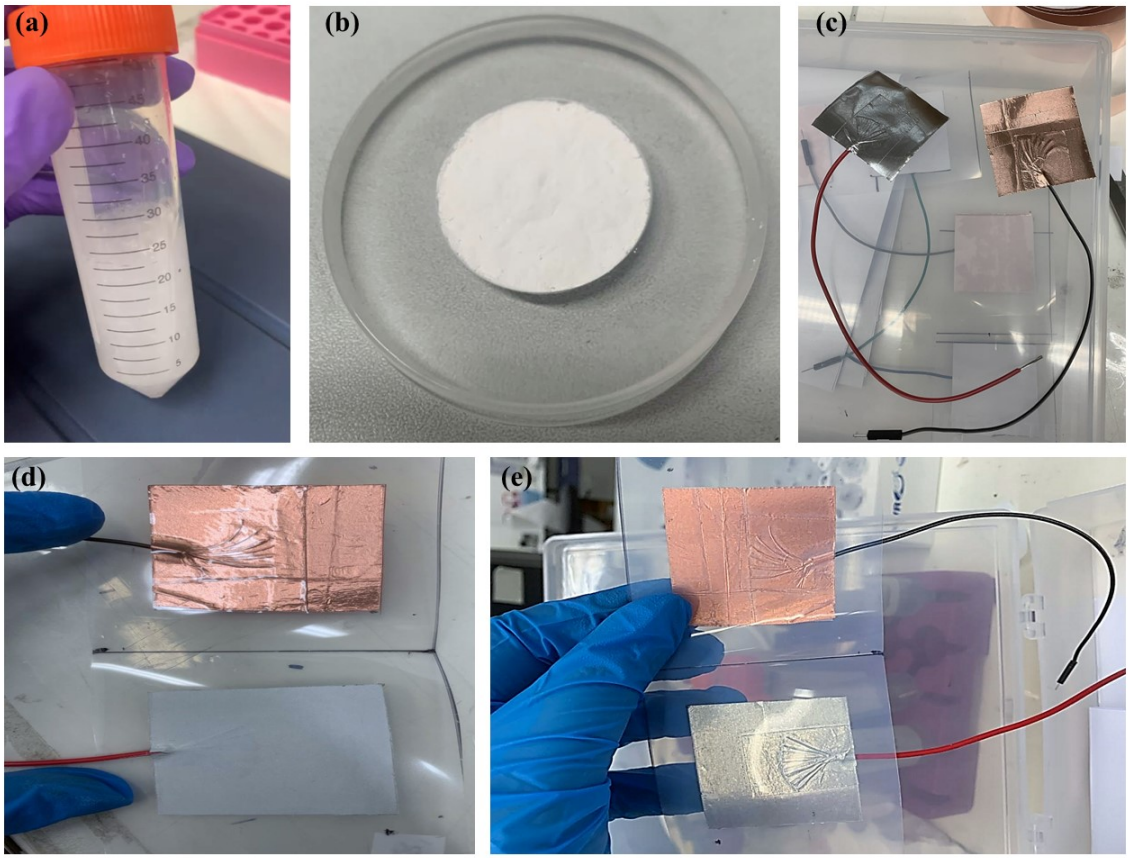

Fig. S1 A photograph depicts **(a)** s-MOF-5 crystals dispersed into ethanol, **(b)** Dried s-Mof-5 powder, **(c)** the two designed electrodes, **(d)** front view and **(e)** the back view of the fabricated TENG device based after adding both the tribopositive and tribonegative layers and the encapsulation using PET.

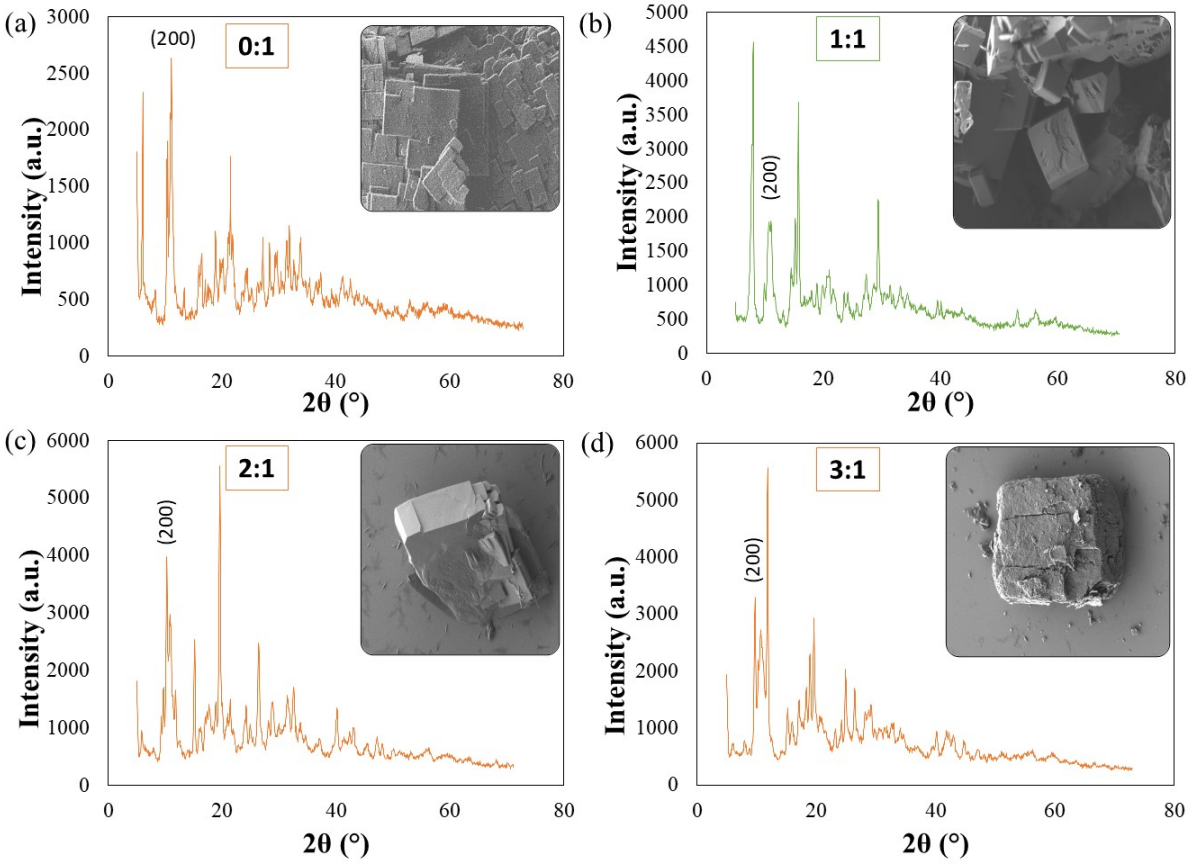

Fig. S2 XRD patterns and corresponding SEM images of surfactant-mediated MOF-5 synthesized using different PEG:DMF ratios: **(a)** 0:1 (no PEG), **(b)** 1:1, **(c)** 2:1, and **(d)** 3:1.

Varying the PEG:DMF ratio revealed that moderate PEG content (1:1) yields the most crystalline and morphologically uniform MOF-5, whereas PEG-free or PEG-rich conditions (0:1 and ≥1:2) induce structural irregularities and reduced crystallinity, confirming 1:1 as the optimal ratio for enhanced porosity and TENG performance.

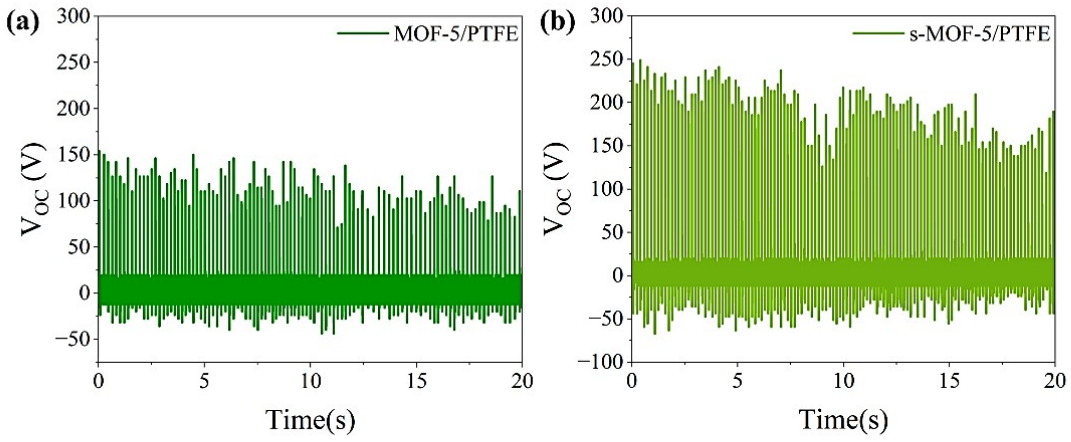

Fig. S3 The open circuit voltage (V_{oc}) *of TENG devices* using PTFE as a tribonegative layer and (a) MOF-5 and (b) s-MOF-5 as tribopositive layer.

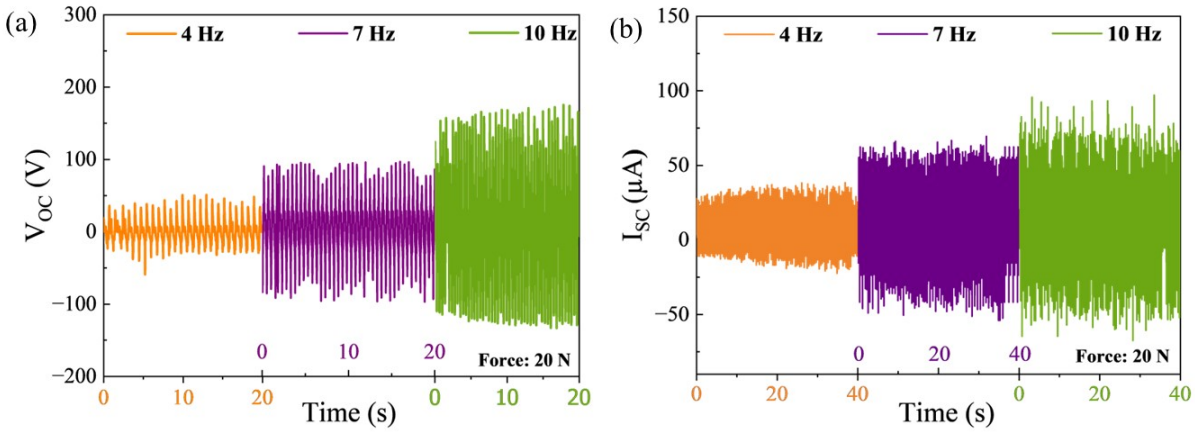

Fig. S4 Output performance of the PEG-mediated MOF-5-based TENG under different operating frequencies (4, 7, and 10 Hz) at a fixed contact force of 20 N: **(a)** short-circuit current (I_{SC}) and **(b)** open-circuit voltage (V_{OC}).

Both I_{SC} and V_{OC} increase with frequency due to the enhanced contact–separation rate, which promotes faster charge accumulation and transfer at the interface. The output reaches a steady maximum at 10 Hz, selected as the working frequency for all subsequent analyses to ensure stable and reproducible signal generation.

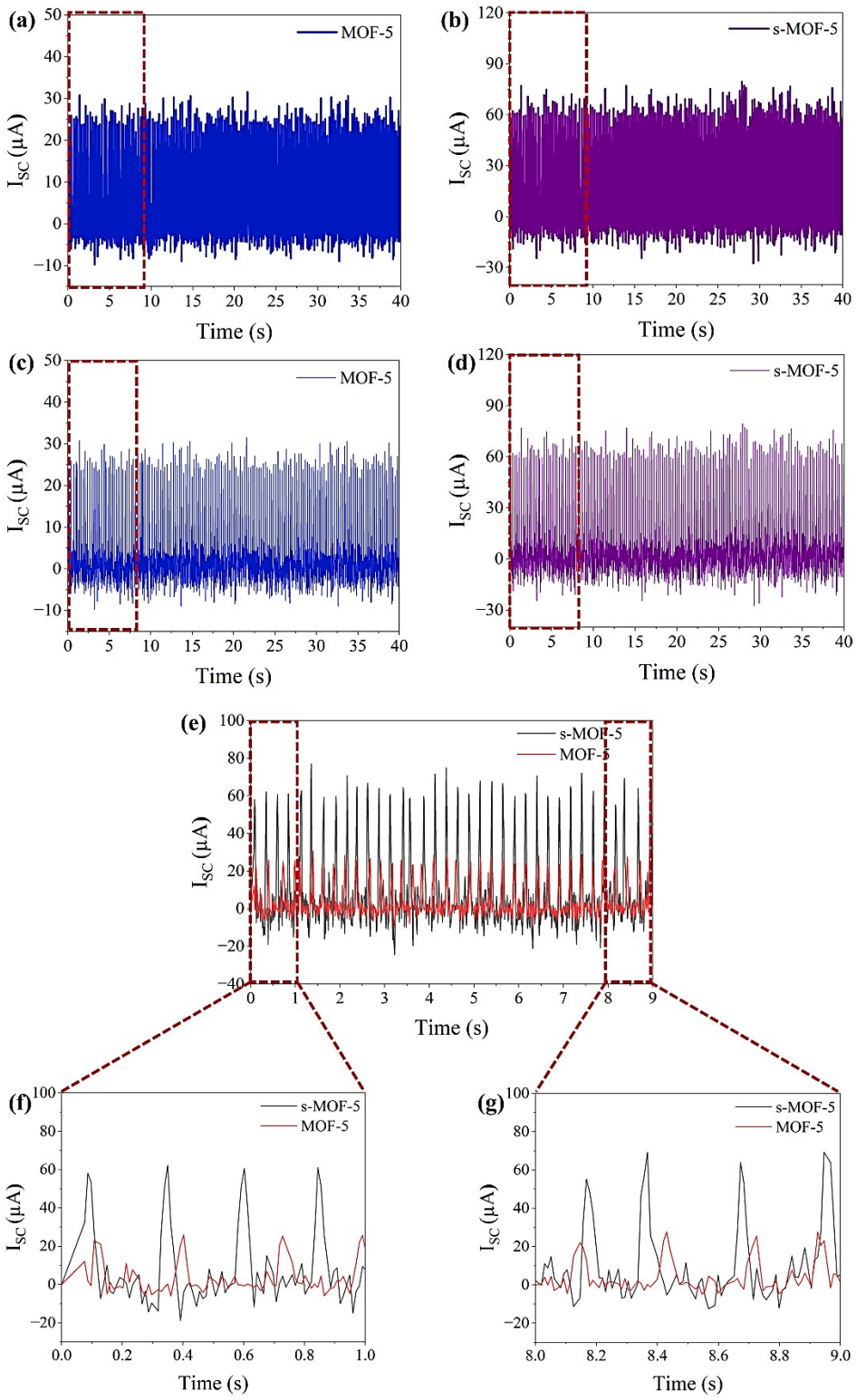

Fig. S5 Comparison of the short-circuit current I_{SC} output signals of **(a)** MOF-5 based TENG with **(b)** s-MOF-5 TENGs at 20 N (10 Hz) and their counterparts with reduced line width **(c)**, **(d)**, respectively. **(e)** A 9-s window for both samples. **(f)** Zoomed-in view of the first 1 s showing distinct pulse shapes and amplitudes. **(g)** Zoomed-in view of the last 1 s showing additional non-identical fluctuations.

Table 1. Statistical comparison of s-MOF-5 and MOF-5 (0–1 s) through a two-sample t-test exported from Origin software.

Descriptive Statistics

		N	Mean	SD	SEM	Median
Current		76	8.04411	20.30107	2.32869	0.81157
C"Current"		76	3.64519	8.31874	0.95422	0.26232
	Difference	76	4.39892		2.51662	-1.00843
	Overall	152	5.84465	15.61868	1.26684	0.50624

Standard Error of Mean (SEM) of difference is computed under the condition that equal variance is assumed.

t-Test Statistics

	t Statistic	DF	Prob>|t|
Equal Variance Assumed	1.74795	150	0.08252
Equal Variance NOT Assumed (Welch Correction)	1.74795	99.49589	0.08356

Table 2. Statistical comparison of s-MOF-5 and MOF-5 (8–9 s) through a two-sample t-test exported from Origin software.

Descriptive Statistics

		N	Mean	SD	SEM	Median
C		81	10.33626	20.30484	2.25609	3.71406
C"C"		81	4.07107	8.18869	0.90985	1.48101
	Difference	81	6.26519		2.43265	1.29455
	Overall	162	7.20366	15.74979	1.23742	1.97692

Standard Error of Mean (SEM) of difference is computed under the condition that equal variance is assumed.

t-Test Statistics

	t Statistic	DF	Prob>|t|
Equal Variance Assumed	2.57546	160	0.01092
Equal Variance NOT Assumed (Welch Correction)	2.57546	105.35191	0.0114

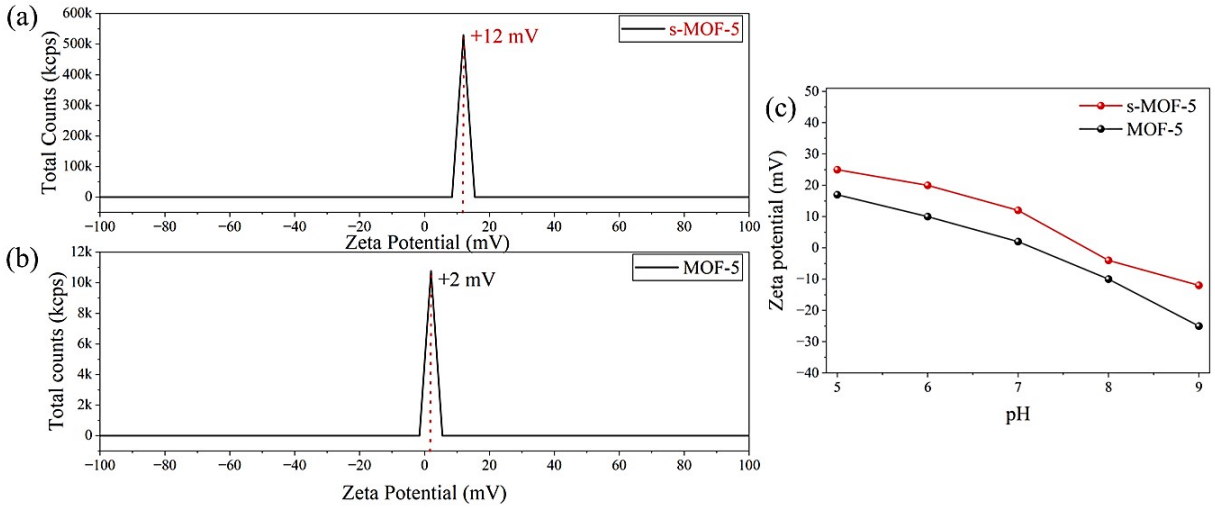

Fig. S6 Zeta potential analysis under neutral pH of 7 for (a) s-MOF-5 and (b) MOF-5. (c) Variation of zeta potentials with pH values for both samples.

Zeta potential measurements have been conducted for both MOF-5 and s-MOF-5. Under neutral pH condition (~7), s-MOF-5 exhibits a more positive ζ-potential (+12 mV) than pristine MOF-5 (+2 mV), as shown in the following Figure S4(a, b). The variation of ζ-potentials under wider range of pH conditions is presented in Figure S4(c). These results prove that surfactant-mediated MOF-5 (s-MOF-5) films are more tribopositive than pristine MOF-5, leading to enhanced charge trapping and overall improved TENG output.

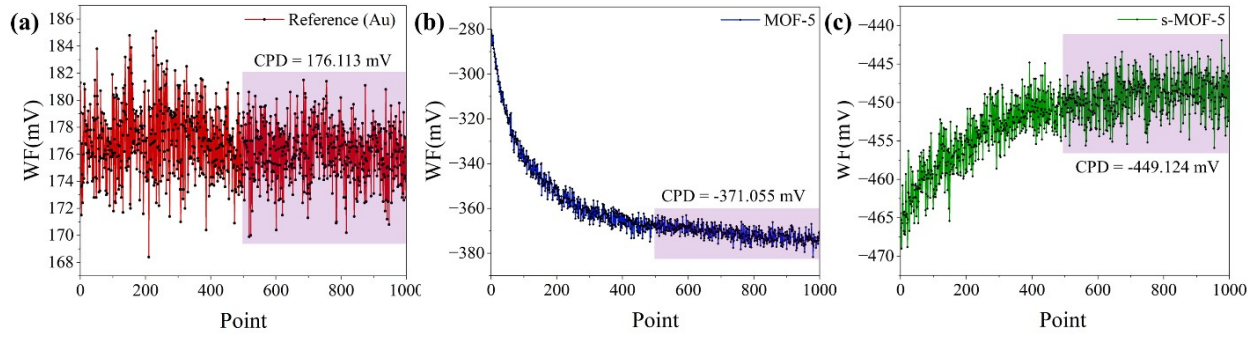

Fig. S7 Kelvin probe measurements of surface potential and the CPD profile of (a) Au reference, (b) pristine MOF-5, and (c) s-MOF-5.

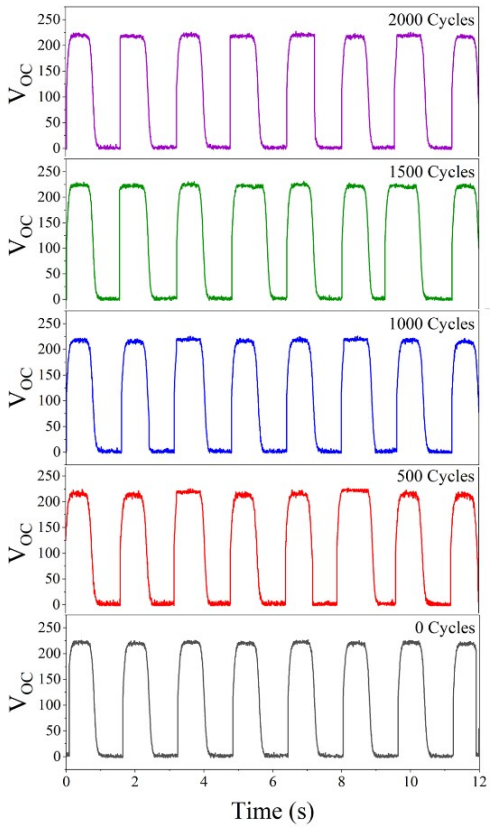

Fig. S8 Output voltage for 2000 bending cycles with a fixed bending angle of about 30° to show the mechanical flexibility and electric stability of the s-MOF-5-based TENG sensor.

The bending stability of the s-MOF-5-based flexible TENG sensor was conducted for 2000 bending cycles with a fixed bending angle of ~30°. As shown in Figure S8, no obvious decay is found in V_{OC}, which is kept at 200–250 V during bending test, showing the excellent stability and flexibility of this TENG device towards bending deformations.

(a)

(b)

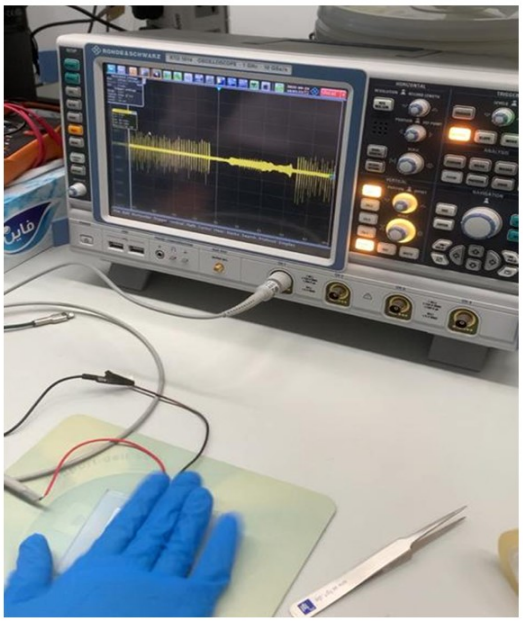

(c)

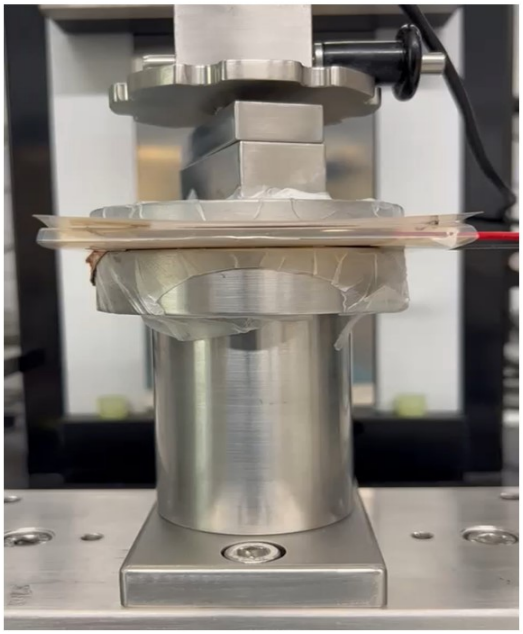

(d)

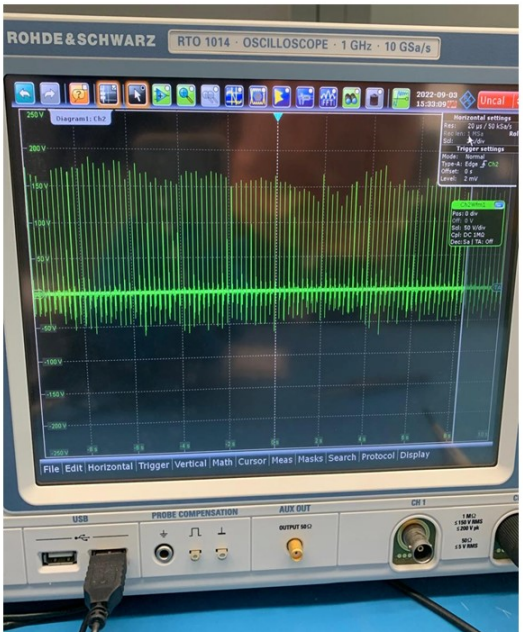

Video TENG Application (Tapping by Hand).mp4 (Co

Video TENG Application (Dampping Video).mp4 (Co

Fig. S9 Videos and photographs illustrate the working mechanism of the as-synthesized MOF-5 triboelectric nanogenerator by repetitively applying **(a, b)** hand force and **(c, d)** using the damping system.